Differential Gain Comparison of Optical Planar Amplifier on Silica Glasses Doped with Bi-Ge and Er, Yb Ions

Jiří Šmejcký* and Vítězslav Jeřábek

Faculty of Electrical Engineering, Technical University in Prague

Abstract: The paper presents the measurement and calculation of the optical amplifier gain and the optimal length of the active optical amplifier waveguide doped with Bi-Ge radiation complexes compared to an optical amplifier with active doping with ions Er^{3+}, Yb^{3+}. At present are using optical amplifiers for the high-capacity optical communication systems in the narrow spectral region of 1530–1560 nm, determined by the gain bandwidth of erbium-doped fiber amplifiers (EDFA) or erbium-doped optical planar amplifiers (EDPA) realized as active planar waveguides in the optical integrated circuits technique. However, it is possible increase wavelength region up to 1610 nm, where optical losses of telecommunication fibers are less than 0.3 dB per km, if appropriate amplifiers are available. In this regard, the development of novel optical amplifiers operating in this spectral region have of great importance. The paper summarizes the results measurement of the attenuation and emission spectra for net gain spectra calculation of the new ion exchange Ag^{+} - Na^{+} optical Er^{3+} and Yb^{3+} doped active planar waveguides realized on silica glass substrates and parameters of novel optical amplifiers for extension of the bandwidth from 1530 to 1610 nm doped by bismuth – erbium ions.

Keywords: Optical waveguides, EDFA, EDPA, BEDF, BAC-Ge, luminescence spectrum.

1. INTRODUCTION

In optical telecommunication systems, optical amplifiers are one of the essential parts of the optical transmission tracts containing silicon fiber waveguides. The main part of optical amplifiers is an optically active fiber waveguide. The information capacity of an optical fiber transmission path is determined by the width of a spectrum of optical amplifiers that use the quantum principle of stimulated radiation and are extensively wave selective. Their selectivity depends on the type of activator that is used to amplify the passing radiation. In order to expand the transmission capacity of the connection, it is necessary to extend the bandwidth of the optical amplifiers. This is possible by using two or more activators in the optical fiber optic amplifier waveguide. In the last few years, several works have been published on broadband fiber active waveguides for optical amplifiers in telecommunication bands. These waveguides contain with erbium and bismuth ions [1], [2] for medium wavelength telecommunication bands at 1340, 1430 and 1700 nm. Broadband optical transmission systems are currently being implemented with parallel optic amplifiers. However, the use of several separate optical amplifiers for broadband telecommunication systems is not optimal, both economically and technically. A more preferable solution would be to use a fiber or planar amplifier with a high bandwidth amplifier, for example for S + C + L (1460 - 1615 nm) or C + L + U (1530 - 1675 nm) bands. Many attempts have been made to achieve optical amplification using erbium and bismuth codoped optical waveguides for broadband near-IR (NIR) band systems. Unfortunately, until now, the continuous spectral range of these materials has not been demonstrated in the desired wavelength range.

The problem is that the typical luminescence spectrum of bismuth and erbium-doped active waveguides has a slight overlap, especially for shorter wavelengths. For this reason, it is not possible to implement a broadband amplifier with a balanced amplification in the band S+C+L (1460-1615 nm), where the overlap of the luminescence spectrum of erbium and bismuth is stronger, see Figure **1**.

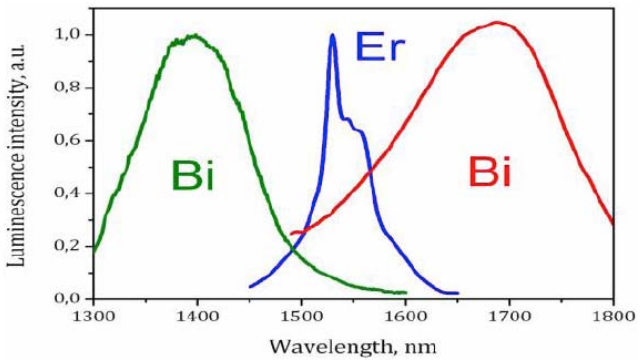

Figure 1: Typical luminescence spectrum of fiber doped with Bi and Er [3].

2. INTRODUCTION TO BROADBAND OPTICAL WAVEGUIDE ISSUES

At present, optical amplifiers for high-capacity optical communication systems in the narrow spectral range of 1530-1560 nm are used, which are determined by the erbium-doped fiber amplification bandwidth (EDFA) or erbium-doped optical planar amplifiers (EDPA) as active planar waveguides in the optical integrated circuits. However, when suitable amplifiers are available, it is possible to increase the range of wavelengths up to 1610 nm, where the optical loss of telecommunication fibers is less than 0.3 dB / km. In this respect, the development of new optical

Address correspondence to this article at the Faculty of Electrical Engineering, Technical University in Prague; E-mail: J.Smejcky@seznam.cz

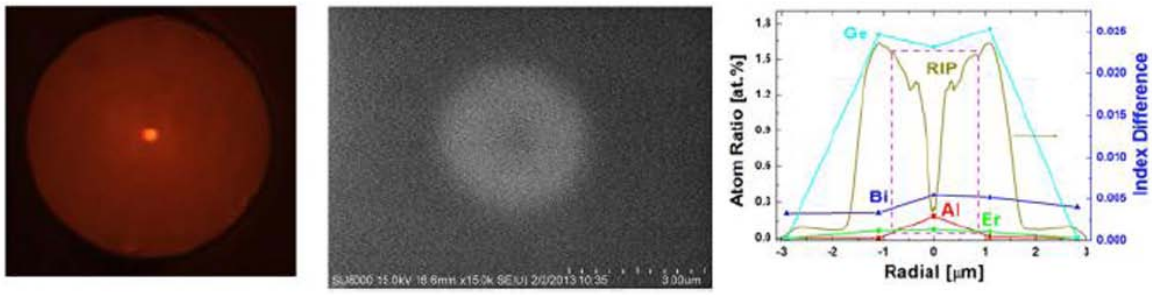

a b c

Figure 2: (a) Cross-sectional image of BEDF; b) image of the BEDF core region SEM; c) BEDF composite radial element and refractive index (RIP) profile (the dashed-line rectangle is the area of impact) [1].

amplifiers operating in this spectral range is of great importance.

In the study of [2], the output optical power of bismuth / erbium doped optical fiber (BEDF) was studied in double pumping at 830 nm and 980 nm. Based on these experiments, the possible energy transitions of the BEDF were proposed. The measurement results demonstrate the benefits of pumping BEDF at 830 nm versus 980 nm in terms of absorption, pumping efficiency, excited state absorption and amplification. Since the first demonstration of broadband emission in glass doped with bismuth [4], attention has increasingly been paid to active Bismuth-doped waveguides for their potential use as active media for broadband amplifiers and super-luminescent sources in the spectral range of 1150–1800 nm. Bismuth-doped waveguides have a wavelength range of 1100-1600 nm. Their fluorescence strongly depends on the wavelength of the pumping radiation because they contain several active centers (bismuth active centers, BACs) with different excitation and emission spectra. This makes it possible to adjust the excitation and emission wavelengths by a type of modifier such as Al, Si, Ge or P. This feature allows you to fine-tune the power of the active bismuth-doped fibres (BDF) by selecting the wavelength of the pumping source. It also shows that BACs are very complicated in nature. It was also shown in [2] that the profile and bandwidth can also be selected and set by the appropriate choice of the source(s) wavelength. Due to the existence of more active bands in the BEDF waveguide, it is advantageous to carry out simultaneous pumping at multiple wavelengths. A comparison of the BEDF power output at the pumping wavelength of 830 nm and 980 nm was made. At that, waveguide attenuation, luminescence properties and on-off gain were measured. By analyzing absorption, amplification, and ESA at 830 nm and 980 nm, two different energy conversion processes were designed and an attempt was made to explain the broadband emission in the BEDF.

2.1. Measurement of the Fiber Waveguide

The research study [1] describes the production of a BEDF waveguide on which the measurement was done, Figure **2**.

In Figure **2a**,**b** is a cross section of the waveguide obtained with a scanning electron microscope. It can be observed that the waveguide can be considered rotationally symmetrical. Figure **2c** is a profile of composite radial element with a plurality of additional dopants (germanium, phosphorus, aluminum, etc.) and wavelength core refractive index waveform (RIP).

2.2. Absorption Spectral Characteristics

On this active optical waveguide, the attenuation was first measured (Figure **3**).

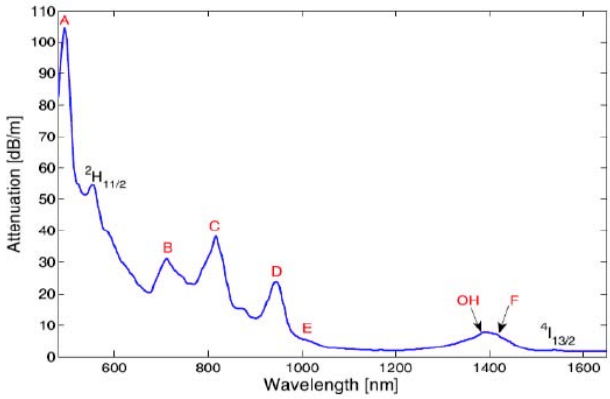

Figure 3: BEDF Attenuation Spectrum [1].

The graph of the spectral damping characteristics shows the spikes at points around 500 (A), 710 (B), 820 (C), 950 (D), 1000 (E) and 1400 nm (F), with peaks of 550 and 1530 nm being attributed to Er^{3+}. Together BAC-Ge, Bi^{2+} and BAC-Si are responsible for the attenuation bands around points A, B, C. Gaussian selection (filtering) distinguished three attenuation zones in the range of 920 to 1100 nm. These are attenuation peaks around wavelengths ~ 950, ~ 980 and ~1020 nm which are attributed to the absorption of BAC-Ge, Er^{3+} and BAC-Al. In addition, there are also

three attenuation bands between 1100 and 1480 nm, which are attenuations at ~ 1350, ~ 1380 and ~ 1410 nm for which BAC-P, OH and BAC-Si are responsible. Spectral Attenuation Characteristics shows the possibility of pumping BEDF at 830 nm (BAC-Si) and 980 nm (BAC-Al and Er^{3+}). Additionally, the attenuation coefficient at 830nm (30.9 dB/m) is approximately four times larger than at 980 nm (7.7 dB /m). It follows that the effective cross section of the absorption at 830 nm is larger than at 980 nm.

2.3. Emission Spectral Characteristics BEDF

The emission spectrum of BEDF excited at 830 nm and 405 nm was measured. The normalized emission spectrum is shown in Figure **4**.

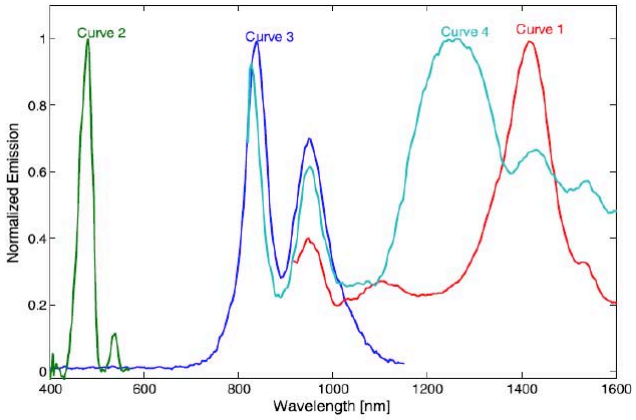

Figure 4: Normalized emission spectra BEDF excited at 830 nm (curve 1 and curve 2) and 405 nm (curve 3 and curve 4) [1].

From the normalized emission characteristics, the existence of the six NIR emission bands (curves 1,3 and 4) occurring around ~ 830,950,1100,1260,1410 and 1530 nm where the first five bands belong to the BAC emission, 1530 nm corresponds to the electron transitions of the erbium ($^4I_{13/2}$ => $^4I_{15/2}$). The emission bands at 830, 1410, 950, 1110 and 1260 nm correspond to BAC-Si, BAC-Ge, BAC-Al and BAC-P. In addition to NIR emissions, two UP-conversions [7] in the bands 480 and 540 nm (curve 2) are identifiable. In addition, the NIR lifetime that is measured at wavelengths 950, 1110, 1260 and 1410 nm is approximately 110,150,450 and 590 µs.

Measuring the life of metastable states corresponds well with the emission spectrum analysis and confirmed the existence of four BACs: BAC-Ge, BAC-Al, BAC-P and BAC-Si. The results of the measurements of the metastasis statuses indicate that the most stable is the metastable state of BAC-Si (590 µs).

Comparison of emission spectral characteristics for single or double pumping. The measurements were made in the arrangement shown in Figure **5**. The measured characteristics are shown in Figure **6**.

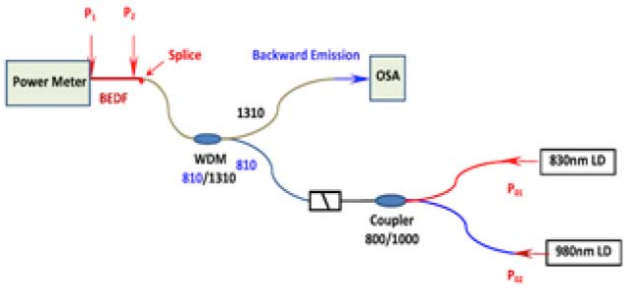

Figure 5: Experimental setup for the back ward emission measurement with 830 nm or 980 nm pumps.

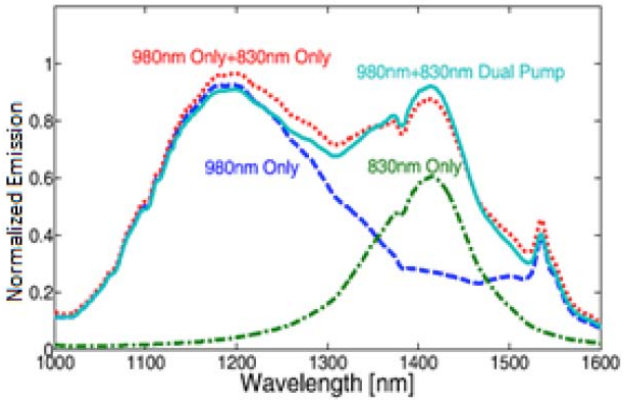

Figure 6: Experimental measurements of emissions while using 830 nm or 980 nm pumps, alternatively and concurrently [1].

In the experimental system, the Optical Spectrum Analyzer (OSA) was used to record backward emission spectra of a 50 cm long BEDF. Laser diodes 830 nm and 980 nm were connected via WDM 800/1000 nm multiplexer to the measured waveguide. The power meter was connected to the output of the waveguide to monitor the residual pumping power for luminescence analysis. From the graph in Figure **6** we can clearly see one emission band at 1410 nm (BAC-Si) when pumping only at 830 nm. When pumping only at 980 nm, there are two emission zones, namely 1190 for BAC-Al and BAC- P and 1536 nm for Er^{3+}. By way of comparison, Figure **6** shows the dependence of the emission on pumping power for pumping wavelengths of 830 nm and 980 nm. It is clear that the emission at 830 nm pumping is growing much faster than when pumping at 980nm.

More detailed information and design of BEDF energy transfer diagram at pumping 980 nm and 830 nm is given in the work [1].

2.4. Optical Amplifier for C+L+U Telecommunication Bands

The results of the experimental measurement by bismuth are remarkable. However, for the third optical

window of quartz waveguides NIR, the band between 1500nm and 1700nm is needed. A fiber amplifier for C+L+U telecommunication area with continuous amplification in the band 1530-1675 nm is described In the study of [3]. In this case, germanosilicate fibers are co-doped with various contents of bismuth and erbium that have been produced by the modified chemical vapor deposition method (MCVD). It should be noted that the BAC emission parameters are strongly dependent on the manufacturing parameters. Therefore, the production of an active optical waveguide with a corresponding Bi / Er ratio is one of the key issues. It is also known that the optical properties of the activated bismuth doped waveguide depend on the chemical composition of the glass from which they are made. An absorbtion spectrum of fibers with different Bi / Er ratios is shown in the picture Figure **7**.

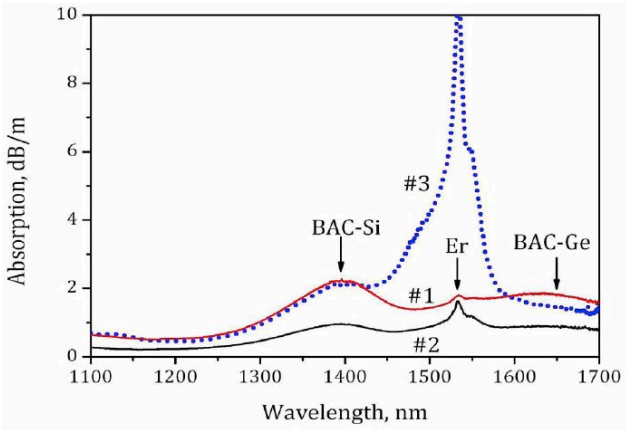

Figure 7: Absorption spectra of the various Bi/Er-codoped germanosilicate fibers [3].

The graphic waveforms exhibit two different absorption peaks at 1650 and 1400 nm, which belong to BAC-Ge and BAC-Si. The absorption band with a peak at 1535 nm is assigned to Er^{3+} ions. It can be seen that the BAC-Ge and Er bands overlap significantly. This fact is also schematically shown in Figure **11**, where the energy levels of Er^{3+} ion and BAC-Ge overlap. Therefore, for the excitation of both active centers, it is possible to use only one source of pumping radiation, in this case at a wavelength of 1460 nm. This is an indisputable advantage over the use of two pumping sources. In this case, when using only one source of pumping radiation at 1460 nm, a continuous gain in the range 1530-1675 nm was achieved, Figure **8**. The technological parameters of the investigated fibers are listed in Table **1**.

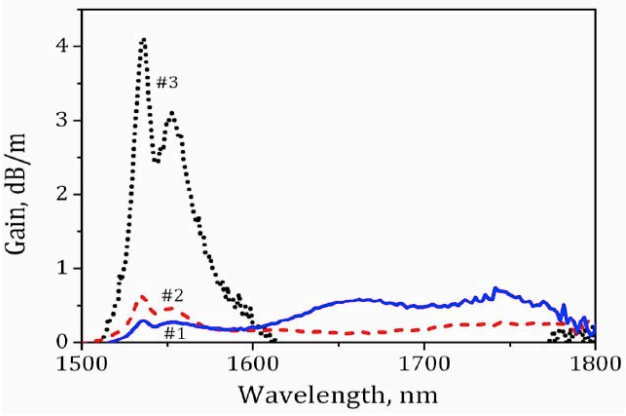

Figure 8: Net gain spectra of the investigated fibers at pumping1460 nm [3].

3. THEORETICAL ANALYSIS OF THE OPTICAL ACTIVE WAVEGUIDE

The theoretical analysis is based on a mathematical model by rate equations, that describes approximately the behavior of the optical active structures (fiber or planar waveguides) and allows to predict theoretically the quantum behavior of the structures and perform some optimizations on technological level. The behavior of the optical active structures is influenced by a number of factors, both the actual composition of the active material and its geometric configuration, the choice of pumping power, the active length of the waveguide. Finding optimal concentrations of activators and precursors is one of the pivotal challenges in the development of optically active structures. At higher concentrations of activators, luminescence is extinguished by clustering of the activator atoms, energy migration or cross-relaxation. The Judd-Ofelt theory is used to assess the influence of matrix atoms on the active ions (activators). However, this optimization is not the subject of this work.

In this work, a mathematical model will be described which allows for the optimization of the length of the active structure and the choice of the pumping power on the basis of solutions of rate equations and equation describing the propagation of the optical signal in the active optical waveguide.

Table 1: The Technological Characteristics of the Fibers [3]

Fiber	Core glass,mol.%	Bi, ppm	Active absorption at 1650 nm, dB m^{-1}	Er,ppm
#1	~50GeO_2- 50SiO_2	140	1.6	15
#2	~50GeO_2- 50SiO_2	150	1.4	100
#3	~50GeO_2- 50SiO_2	150	0,85	1500

The calculation of the amplification of the optical active waveguide essentially resides in the solution of the system of differential equations describing the occupation of atomic levels (the so-called rate equations) and in the solution of propagation of light by the propagation equation. Differential rate equations are derived from three basic phenomena describing the probability of the transition of the quantum system: spontaneous emission, stimulated emission and absorption. The energy gradients in the erbium-ytterbium complex are described by absorption and emission effective cross-sections. For insulated non-degraded atoms, the following applies: $\sigma_e(\nu) = \sigma_a(\nu) = \sigma(\nu)$. In the real system, however, the energy levels are always degenerated and therefore the absorption and emission spectral waveforms differ: $(\sigma_e(\nu) \neq \sigma_a(\nu))$.

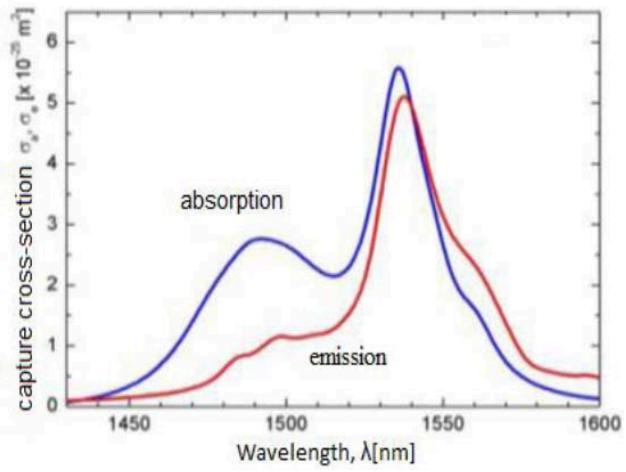

Figure 9: Absorption and emission cross-section spectrum of the silica waveguide Er^{3+} [5,7].

3.1. Rate Equations for Three-Level System for Er and Yb

The Erbium-Ytterbium complex can roughly be described as a three-level quantum system (1) - (3) using rate equations in the form:

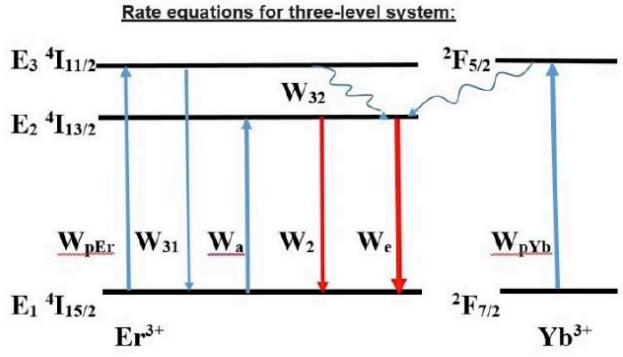

Figure 10: Erbium-Ytterbium complex can roughly be described as a three-level quantum system.

$$\frac{dN_3}{dt} = -W_{32}N_3 - W_{31}N_3 + W_{pEr}N_1 \quad (1)$$

$$\frac{dN_2}{dt} = W_{32}N_3 - W_2N_2 - W_e N_2 + W_aN_1 + W_pN_1 \quad (2)$$

$$N_{tot}^{Er+Yb} = N_1 + N_2 + N_3 = N_{tot} \quad (3)$$

Where:

N_1, N_2, N_3 are the numbers of excited ions in a unit volume (ion concentration) at 1,2,3 levels N_{tot} is the total number of excited ions in a unit volume

W_{32} is the rate coefficient of non-radiation transition from E_3 to E_2

W_{31} is the rate coefficient of non-radiation transition from E_3 to E_1

$W_2 = \frac{1}{\tau_2}$ is spontaneous emissions (4)

$W_p = \frac{I_p}{h\nu_p}(\sigma_{pEr} + \sigma_{pYb}) = W_{pEr} + W_{pYb} = \frac{I_p}{h\nu_p}\sigma_p$ is the (5)

rate coefficient pumped

$W_a = \frac{I_s}{h\nu_\lambda}\sigma_{aEr}$ is the rate coefficient of stimulated (6)

absorption

$W_e = \frac{I_s}{h\nu_\lambda}\sigma_{eEr}$ is the rate coefficient of stimulated (7)

emission

I_p, I_s, is intensity of pumping and signal radiation

σ_{pEr} , σ_{aEr} , σ_{eEr} are the pumping, absorption and emission effective cross sections for erbium

h is Planck's constant

In a three-level system, the highest level of E3 together with the base level E1 forms the transition allowing the absorption of exciting radiation. After E3 excitation, the quantum system is ideally switched to E2 immediately. Thus, the E3 level is practically zero, and since it does not directly participate in the amplification of the signal, it is not considered in the model described below.

For $N_3 = 0$ it is possible formulate (8) and (9)

$$\frac{dN_2}{dt} = W_pN_1 + W_aN_1 - W_2N_2 - W_e N_2 \quad (8)$$

$$N_{tot}^{Er+Yb} = N_1 + N_2 = N_{tot} \quad (9)$$

Static solution of rate equations

$$N_2 = \frac{(W_p + W_a)N_{tot}^{er}\tau_2}{1 + \tau_2(W_p + W_a + W_e)} \quad (10)$$

Equation (11) of optical signal propagation by optical waveguide

$$\frac{dI_S(z)}{dz} = I_s\ (\sigma_e(\nu)N_2 - \sigma_a(\nu)N_1) \quad (11)$$

Equation (12) of propagation of pumping radiation:

$$\frac{dI_p(z)}{dz} = \sigma_e(\nu)N_1 I_p \quad (12)$$

In general is : $I(z) = \frac{P(z)}{S} = \frac{P(z)\Gamma}{\pi r^2}$ (13)

It is advantageous to describe the signal gain in the waveguide by optical power P(z) rather than intensity:

$$P(z) = I(z)\pi r^2/\Gamma \quad (14)$$

In addition, the resulting relationships for calculating the waveguide gain are given depending on its length and the required pumping power that were derived under certain simplified assumptions.

Rate equations: $\frac{N_2}{N_t} = \frac{\sum_\lambda \frac{P_\lambda(z)\alpha_\lambda}{h\nu\xi}}{1+\sum_\lambda \frac{P_\lambda(z)\,(\alpha_\lambda + g_\lambda)}{h\nu\xi}}$ (15)

$\alpha_\lambda = \sigma_{a,\lambda}\Gamma_\lambda N_t,\ g_\lambda = \sigma_{e,\lambda}\Gamma_\lambda N_t$ where N_t is average (16)

concentration of doping

where α_λ , g_λ are coefficients of attenuation and gain.

Γ_λ is the overlap integral (overlap factor – does not depend on z) with which the effective average radiation intensity in the doped activator region can be expressed.

The gain of a waveguide $G_{dB}(\lambda)$ in [dB] depending on its length is described by equation (17):

$$G_{dB}(\lambda) = 10log_{10}(e)\ [(\alpha_\lambda + g_\lambda)\frac{N_2}{N_{tot}} - (\alpha_\lambda + \alpha_{\lambda 0})]\cdot L \quad (17)$$

The gain $G_{dB}(\lambda)$ of the waveguide expressed by the Wa, We, Wp rate coefficients is given by the equation (18)

$$G_{dB}(\lambda) = 10\ log_{10}(e)\ [(\alpha_\lambda + g_\lambda)\frac{W_a + W_p}{\frac{1}{\tau_2} + W_p + W_a + W_e} - (\alpha_\lambda + \alpha_{\lambda 0})]\cdot L \quad (18)$$

3.2. Rate Equations for Three-Level System for Er^{3+} Ions and BAC-Ge

Figure **11** shows a possible arrangement of a three-level energy system of the Er and BAC-Ge complex. It is known that the optical properties of bismuth-doped glass strongly depend on the chemical composition of the glass resp. on the modifiers used, which in this case were Ge and Si. In particular, the absorption band BAC-Ge significantly overlaps with the absorption band Er^{3+}. Thanks to this overlap, it is possible to excite both active centers by pumping at one wavelength of 1460 nm. During this excitation, which falls into the two corresponding absorption bands shown in Figure **11** (right), Er^{3+} and BAC-Ge simultaneously fill the metastable $^4I_{13/2}$ level and the E2 level. This is an indisputable advantage compared to a situation where two pumping sources are required.

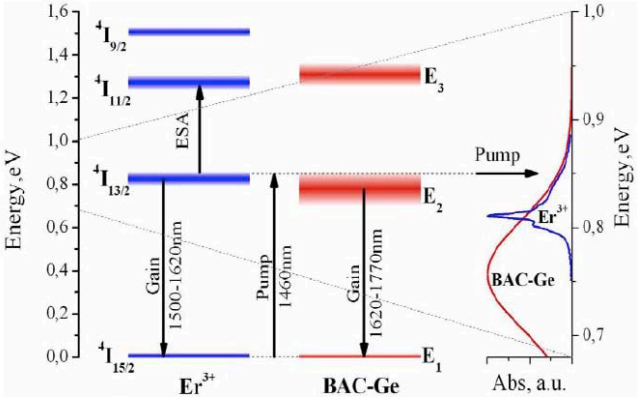

Figure 11: Energetic levels of Er^{3+} and BAC-Ge. Absorption bands Er^{3+} and BAC-Ge (right) [3].

The Er^{3+} and BAC-Ge complex can roughly be described as a three-level quantum system using rate equations (17) – (19) in the form:

$$\frac{dN_3}{dt} = -W_{32}N_3 - W_{31}N_3 + W_p N_1 \quad (19)$$

$$\frac{dN_2}{dt} = W_{32}N_3 - W_2N_2 - W_{eEr}N_2 - W_{eBAC-Ge}N_2 + + W_{aEr}N_1 + W_{aBAC-Ge}N_1 + W_pN_1 \quad (20)$$

$$N_{tot}^{Er+BAC-Ge} = N_1 + N_2 + N_3 = N_{tot} \quad (21)$$

where W_{32} is the rate coefficient of non-radiation transition from E_3 to E_2 ,

W_{31} is the rate coefficient of non-radiation transition from E_3 to E_1,

$W_2 = \frac{1}{\tau_2}$ is coefficient spontaneous emission, (22)

$W_p = \frac{I_p}{h\nu_p}(\sigma_{pEr} + \sigma_{pBAC-Ge}) = W_{pEr} + W_{pBAC-Ge} =$

$\frac{I_p}{h\nu_p}\sigma_p$ is the rate pumping coefficient, (23)

$W_{aEr} = \frac{I_S}{h\nu_\lambda}\sigma_{aEr}$ is the rate coefficient of stimulated absorption Er, (24)

$W_{aBAC-Ge} = \frac{I_S}{h\nu_\lambda}\sigma_{aBAC-Ge}$ is the rate coefficient of stimulated absorption BAC-Ge, (25)

$W_{eEr} = \frac{I_S}{h\nu_\lambda}\sigma_{eBAC-Ge}$ is the rate coefficient of stimulated emission Er, (26)

$W_{eBAC-Ge} = \frac{I_S}{h\nu_\lambda}\sigma_{eBAC-Ge}$ is the rate coefficient of stimulated emission BAC-Ge. (27)

To calculate the BAC emission sections, Fuchtbauer-Ladenburg [2] proposed a relationship

based on the fact that stimulated emission cross section $\sigma(\lambda)$ as a function of wavelength to a first approximation coincides with the spontaneous emission spectrum, which is expressed by the following formula (28),

$$\sigma(\lambda) = \frac{\lambda^2 g(\lambda)}{8\pi n^2 \tau} \quad (28)$$

where λ is wavelength, $g(\lambda)$ is the normalized spontaneous emission shape function, n is the host refractive index, and τ is the emission lifetime.

By assuming a Gaussian-shaped emission band, the stimulated emission cross section σ at the band center can be estimated by the following formula (29)

$$\sigma(\lambda) = \frac{\lambda^2}{4\pi n^2 \tau \Delta\nu}\sqrt{\ln 2/\pi} \quad (29)$$

Where

$\boldsymbol{\lambda}$ is the central wavelength of the BAC emission band,

$\Delta\nu$ is the width of the BAC emission band,

$\boldsymbol{\tau}$ is the lifetime of BAC luminescence,

n is the core refractive index of the waveguide core.

As in the previous case, it is possible express the gain $G_{dB}(\lambda_{Er})$ by (30), (31) for for active waveguide Er^{3+} ions and gain $G_{dB}(\lambda_{BAC-Ge})$ for BAC-Ge by (32), (33)

$$G_{dB}(\lambda_{Er}) = 10\log_{10}(e)\ [(\ \alpha_{\lambda Er} + g_{\lambda Er})\frac{N_2}{N_t} - (\alpha_{\lambda Er} + \alpha_{\lambda 0Er})] \cdot L \quad (30)$$

The gain $G_{dB}(\lambda_{Er})$ of the waveguide expressed by the W_{aEr}, W_{eEr}, W_{pEr} rate coefficients is given by (29),

$$G_{dB}(\lambda_{Er}) = 10\log_{10}(e)\ [(\ \alpha_{\lambda Er} + g_{\lambda Er}).\ \frac{W_{aEr} + W_{pEr}}{\frac{1}{\tau_2} + W_{pEr} + W_{aEr} + W_{eEr}} - (\alpha_{\lambda Er} + \alpha_{\lambda 0Er})] \cdot L \quad (31)$$

and for BAC-Ge by (30)

$$G_{dB}(\lambda_{BAC-Ge}) = 10\log_{10}(e)\ [(\alpha_{\lambda BAC-Ge} + g_{\lambda BAC-Ge})\frac{N_2}{N_t} - (\alpha_{\lambda BAC-Ge} + \alpha_{\lambda 0BAC-Ge})]\cdot L \quad (32)$$

The gain of the waveguide expressed by the $W_{aBAC-Ge}$, $W_{\mathrm{eBAC-Ge}}$, $W_{\mathrm{pBAC-Ge}}$, rate coefficients is expressed by (31)

$$G_{dB}(\lambda_{BAC}) = 10\log_{10}(e)\ [(\ \alpha_{\lambda BAC-ge} + g_{\lambda BAC-Ge})\ \frac{W_{aBAC-Ge} + W_{pBAC-Ge}}{\frac{1}{\tau_2} + W_{pBAC-Ge} + W_{aBAC-Ge} + W_{eBAC-Ge}} - (\alpha_{\lambda BAC-Ge} + \alpha_{\lambda 0BAC-Ge})]\cdot L \quad (33)$$

L is the length of the active waveguide

These relationships apply approximately results, the exact solution requires a numerical solution of the mathematical model (17) – (19). However, the approximate solutions and simplicity of the calculation

Table 2: Emission Parameters of Luminescence Spectra Under Single 830 nm, 980 nm and 1480 nm Pumping

Pump	**BAC-Al**	**Δv**	**τ**	**$\sigma_{e\text{-}Al}$**
[nm]	**[λ_c - nm]**	**[nm]**	**μs**	**cm^2**
830	1100	193.1	460	2.81×10^{-21}
980	1125	202.5	844	1.70×10^{-21}
1480	. . .	. . .	. . .	. . .
Pump	**BAC-P**	**Δv**	**τ**	**$\sigma_{e\text{-}P}$**
[nm]	**[λ - nm]**	**[nm]**	**μs**	**cm^2**
830	1315	131.9	564	2.3×10^{-21}
980	1350	200.2	624	3.2×10^{-21}
1480	. . .	. . .	. . .	. . .
Pump	**BAC-Si**	**Δv**	**τ**	**$\sigma_{e\text{-}Si}$**
[nm]	**[λ - nm]**	**[nm]**	**μs**	**cm^2**
830	1425	110.7	626	2.1×10^{-21}
980	. . .	. . .	. . .	. . .
1480	. . .	. . .	. . .	. . .
Pump	**BAC-Ge**	**Δv**	**τ**	**$\sigma_{e\text{-}Ge}$**
[nm]	**[λ - nm]**	**[nm]**	**μs**	**cm^2**
830	1430	180	530	3.9×10^{-21}
980	1560	190	540	4.8×10^{-21}
1480	1610	240	490	7.6×10^{-21}

Table 3a: Measured and Calculated Gain of Active Waveguide with Doping Parameters # 1

fiber #	wavelength λ[nm]	G_{meas} [db/m]	G_{calc} [dB/m]	Deviation G_d[dB]
#1	1535	0,4	0,48	-0,08
#1	1550	0,3	0,4	-0,1
#1	1600	0,2	0,25	-0,05
#1	1675	0,6	0,49	0,11
#1	1700	0,55	0,85	-0,3

Table 3b: Measured and Calculated Gain of Active Waveguide with Doping Parameters # 2

fiber #	wavelength λ[nm]	G_{meas} [db/m]	G_{calc} [dB/m]	Deviation G_d[dB]
#2	1535	0,65	0,71	-0,06
#2	1550	0,51	0,64	-0,13
#2	1600	0,2	0,15	0,05
#2	1675	0,16	0,15	0,01
#2	1700	0,2	0,35	-0,15

Table 3c: Measured and Calculated Gain of Active Waveguide with Doping Parameters # 3

fiber #	wavelength λ[nm]	G_{meas} [db/m]	G_{calc} [dB/m]	Deviation G_d[dB]
#3	1535	4,1	3,7	0,4
#3	1550	2,7	2,4	0,3
#3	1600	0,2	0,1	0,1
#3	1675	. . .	-0,02	. . .
#3	1700	. . .	-0,7	. . .

are very useful. The measured and calculated gain of the active waveguide with doping parameters # 1, # 2, # 3 are shown in Tables **3a**, **3b**, **3c**.

4. CONCLUSION

The article summarizes the existing knowledge about the principles and properties of active waveguides doped with bismuth (Bi) and erbium (Er3 +). Germaniun was used as a modifier in the case of bismuth, which forms a BAC-Ge complex with bismuth. Furthermore, a simplified mathematical model for calculating the gain of active waveguides was developed. It is known [3] that bismuth with an admixture of germanium forms a BAC-Ge complex, whose luminescence spectral characteristic overlaps with the spectral characteristic of erbium and extends it to the longer wavelength range (NIR). This modified structure makes it possible to build ultra-wideband optical amplifiers with a large bandwidth of up to 250 nm in the area of the third optical attenuation window of silica waveguides. Since bismuth is a transition metal with external d orbitals, it easily interacts with the environment (with matrix atoms). Unlike rare earth elements, where optically active orbitals are well isolated, there is a much greater influence of the surrounding matrix on broadband radiation than in erbium itself. Thus, it is clear that the adjustment of the concentration of individual dopants and modifiers as well as the material of the matrix itself is of key importance for the resulting spectral characteristics of the active waveguide thus formed. As can be seen in [3], the Er^{3+} and BAC-Ge activators can be pumped at a single wavelength of 1460 nm. Thus, a broadband amplifier with such a doped active waveguide can be pumped by a single source of pump radiation (pump), which is an indisputable advantage. In addition to using germanium as a modifier, other elements such as silicon, aluminium and phosphorus were tested. However, for telecommunication use in the C+L+U band, the use of germanium as a modifier appears to be most advantageous. The profit values given in the cited publication were verified on our mathematical model. The calculation shows a good agreement between the measured and calculated profit values (Table **3**). The differences between the measurements

and the results from our numerical model were up to 10%. The most balanced spectral characteristic was calculated for the dopant concentrations Er (15 ppm) and Bi (140 ppm), where an average gain of 0.4 dB /m was achieved. If the length of the active waveguide is 50 meters, then the total gain of the amplifier will be up to 20 dB.

ACKNOWLEDGEMENT

Our research is supported by the Student Grant Competition of the Czech Technical University in Prague under grant number SGS16/162/OHK3/2T/13.

REFERENCES

[1] Yan B, Luo Y, Zareanborji A, Xiao G, Peng G-D, Wen J. Performance comparison of bismuth/erbium co-doped optical fiber by 830 nm and 980 nm pumping. Journal of Optics 2016; 18: 1-9. https://doi.org/10.1088/2040-8978/18/10/105705

[2] Zhao Q, Luo Y, Wang W, Canning J, Peng G-D. Enhanced broadband near-IR Luminescence and gain spectra of bismuth/erbium co-doped fiber by 830 and 980 nm dual pumping. AIP Advances 2017; 7: 045012. https://doi.org/10.1063/1.4981903

[3] Firstov SV, Riumkin KE, Khegai AM, Alyshev SV, Mekumov MA, Khopin VF, Afanasiev FV, Dianov EM. Widebannd bismuth and erbium codoped optical fieber amplifier for C + L + U telecommunication band. Laser Phys Lett 2017; 14: 110001. https://doi.org/10.1088/1612-202X/aa8adf

[4] Murata K, Fujimoto Y, Kanabe T, Fujita H, Nakatsuka. Bi-doped SiO2 as a new laser material for an intense laser. Fusion Eng Des 1999; 44: 437-9. https://doi.org/10.1016/S0920-3796(98)00334-2

[5] Smejcky J, Jerabek V, Nekvindova P. Gain Determination of Optical Active Doped Planar Waveguides, Conference: Conference on Photonics, Devices, and Systems VII, Prague, AUG 28-30, 2017, Proceedings of SPIE, Volume: 10603, Article 106030P. https://doi.org/10.1117/12.2294030

[6] Smejcky J, Jerabek V. Nekvindova, Wideband Bismuth – Erbium Doped Optical Active Planar Waveguides, Proceedings OK 2018 Prague.

[7] Michel JF. Digonnet, Rare-Earth-Doped Fiber Lasers and Amplifiers. Second Edition, Revised and Expanded.

Received on 04-10-2020 Accepted on 15-11-2020 Published on 10-12-2020

DOI: https://doi.org/10.31875/2410-4701.2020.07.08